Design and Analysis of Supersonic Inlet for Ramjet Engines: Aerodynamic Considerations and Performance Optimization

Mohammad Hossein Moghimi EsfandAbadi, Adnan Mohammadi, Mohammad Hassan Djavareshkian

1- Abstract

This research delves into the intricate realm of supersonic inlet design for ramjet engines, honing in on the critical aerodynamic considerations and optimization of performance factors. At Mach 2.5, the study meticulously scrutinizes pivotal design parameters, including the placement and number of inclined shocks, cowl-lip positioning, throat area, spike location, and diffuser length. Computational fluid dynamics (CFD) simulations are harnessed to unravel the intricate flow dynamics and assess the proposed inlet geometry's performance.The findings reveal a nuanced relationship between back pressure and shock wave positioning, where increasing back pressure initiates a shift in the shock wave, impacting the flow state. The paper delineates this transition, emphasizing the pivotal back pressure range of 300,000 to 350,000 pascals, where optimal shock wave alignment corresponds with design parameters, achieving a supercritical state. However, elevating back pressure beyond this range triggers a subcritical state and mass flow overflow as the shock exits the throat. Furthermore, the study explores various performance metrics, encompassing drag coefficient, distortion coefficient, mass flow ratio (MFR), and total pressure recovery (TPR) under varying back pressure conditions. The outcomes underscore the merits of higher back pressures, which mitigate drag coefficient and distortion while amplifying TPR. In the subcritical state, MFR diminishes due to shock wave displacement beyond the intake opening.This research illuminates the intricate dance of aerodynamics within ramjet engine inlets and underscores the paramount significance of optimizing inlet geometry to unlock heightened performance. It effectively encapsulates the essence of the full article, enticing readers to embark on a deeper exploration of this crucial area of aerospace engineering.

Keywords: Ultrasonic air intake, Flow Separation, Total Pressure Recovery, Mass Flow Ratio, Designing, numerical simulation

Article Highlights :

- Supersonic inlet design impacts ramjet engine performance.
- Back pressure crucial for shock wave positioning.
- Optimization enhances drag reduction and pressure recovery.

Nomenclature

a_∞ = Free Stream Sound Speed

C_d = Drag Coefficient

FD = Distortion Factor

h = Flight Height(m)

M = Inlet Mach

M_e = Outlet Mach

MFR= Mass Flow Ratio

$\dot{M}$ = Mass Flow (Kg/s)

P_∞, P, P_t = Free Flow pressure, Static pressure, Total pressure(Pa)

R= Universal Gas Constant

T_∞, T, T_t = Free Flow Temperature, Static Temperature, Total Temperature(K)

TPR=Total Pressure Recovery

Greek symbols

ρ_∞ = Free Flow Density

β =Shock Wave Angle (Degree)

θ =Deflection Angle (Degree)

δ = Cone Angle (Degree)

γ = ratio of specific heat for air

2-Introduction

Today, the use of supersonic inlet for ramjet engines and investigation of shock wave are the main interests in aviation devices[1-8]. Therefore, this section undertakes a comprehensive review of research conducted in this domain.Inflow aerodynamics was developed during World War II and simultaneously with the development of jet engines. Realizing the advantage of supersonic flights in the late 1940s led to the development of research in the field of inlet design. This research is based on investigating the effects of the efficiency of shock wave systems as a flow condenser, the necessary matching between the external and internal flow, and exploring the impact of The flight height and the local flow areas in the design [9]. In air-breathing supersonic rockets, the oxygen required for combustion is supplied from the surrounding air. In pneumatic propulsion systems, the inlet opening is critical because it primarily compresses the air. In turbojet engines, air compression is done by the compressor, but in ramjet engines, which do not have a compressor, this task is entrusted to the intake port. When the flow passes through the vertical shock, the static pressure drops increase rapidly as the Mach number increases. Therefore, for high Mach numbers, using an orifice with a single vertical shock is not reasonable. Slowing down the flow through a series of oblique shocks is better. In this method, the flow passes through successive stages of condensation, and finally, a vertical shock is created at the minimum possible Mach number. In other words, the flow compression process is done in several consecutive steps [10]. The compression process occurs through several shock waves produced by the external compression surfaces and the cowl. Subsequently, the internal compression surfaces generate additional shock waves that move from the cowl lip toward the inner section of the engine face [11]. Most of the computations reported in the literature are for supersonic combustion chambers and scramjet inlets [12]. The shape of these inlets is relatively simple since normal shocks cause no significant changes in flow. In contrast, the flow through ramjet inlets undergoes multiple oblique shocks before being converted to subsonic flow by a terminating normal shock. Subsequently, the flow is directed into the combustion chamber. Ramjet inlets are more complex due to a terminal normal shock. Combustion processes are introduced into the ramjet inlets by maintaining a higher back pressure [13]. Light Hill theoretically investigated the ultrasonic flow around rotating bodies. Conroe Meyer studied the design criteria of two-dimensional and axially symmetrical inputs and outputs . Stitt and Salmi experimentally investigated the performance of an axially symmetric mixed compression type duct for Mach 2.5 to 3 and concluded that The peak recovery was increased at Mach 3.0 from 83 to 87 percent with an additional 7.5

percent bleed in t h e subsonic diffuser. At Mach 2.0, an extra 3 percent bleed i n the diffuser increased the recovery from 90.5 to 93.5 percent[14].In 1981, Syberg et al. studied and investigated the technology of making an ultrasonic intake[15].In 1986, Holt and Hunter investigated the ultrasonic duct under angle of attack using Navier-Stokes equations and presented that Both center body and internal cowl computed static pressures agreed well with experimental data[16]. Rodrigues has done a multi-objective optimization of an ultrasonic duct using numerical solution (CFD)[17]. Cole Will Starkey et al. presented an axially symmetric supersonic inlet design for a hybrid motorcycle, based on the SR-71 engine inlet design, in 2006[18].In 2007, Yusuke et al. presented studies on the effect of changing the geometry of axially symmetric inlets on their performance[19].In the 40s and 50s, the two issues of investigating the spillage and shock wave oscillation in air intake ducts were considered, and then in the late 60s, the issue of dynamic disturbances, and in the late 70s, the case of rotation, which is limited to a specific group of ducts, was considered[20].In 1998, Lu and Jain numerically investigated the subject of shock wave oscillation in the air duct[21]. The method of calculating the external Drag and pressure recovery of air ducts with a conical middle body three was also reviewed and presented by Goldsmith and Griggs in 1953[22]. Reno and Maurice demonstrated a two-dimensional ultrasonic duct design method with the criterion of maximum total pressure recovery theoretically and experimentally in 2005[23]. Experimental and computational investigation of the effect of angle of attack on the performance of a rectangular supersonic intake for the High-Mach Integrated Control Experiment (HIMICO). Results show that a positive angle of attack increases mass capture ratio and total pressure recovery but also eases the transition to intake buzz. A model is created to estimate the buzz transition point based on pseudo-shock wave characteristics. However, the method of designing is crucial, and considered as a part of exploring is not investigated [24]. Flow instabilities are investigated experimentally and computationally in a supersonic intake with a ramp-isolator configuration. Results show shock oscillations, boundary layer fluctuations, and their interplay cause buzz, rotating stall, and inlet unstart. The ramp-isolator junction impacts shock/boundary layer interactions, with a smoothed junction reducing instabilities. Overall, the work provides insight into intake instability mechanisms. While the significance of intake design stages holds particular importance in the studies within this field, comprehensive details pertaining to this critical issue have not been delineated [25]. performance of a supersonic axisymmetric external compression air intake at off-design conditions is computationally investigated. By varying the position of the central body, the shock wave system is optimized to maximize total pressure recovery. Results show the intake operates optimally around Mach 2 rather than the design point of Mach 2.5. Although an inquiry into fundamental design parameters, such as mass flow ratio (MFR) and total pressure recovery (TPR), has not been conducted [26].

The purpose of this research is the preliminary aerodynamic design of the entry duct of a ram jet that flies at Mach 2.5 under the design conditions. This duct has a cone-shaped ramp as a supersonic diffuser, responsible for compressing the supersonic flow, and a subsonic diffuser. The sound is responsible for the continuation of the flow compression after passing through the throat of the conduit.

3-Statement of the Problem:

The problem addressed in this research is the design optimization of supersonic inlets for ramjet engines operating at Mach 2.5. The study focuses on the critical aerodynamic considerations and the optimization of performance factors to achieve heightened engine performance. The key design parameters investigated include the placement and number of inclined shocks, cowl-lip positioning, throat area, spike location, and diffuser length. The specific challenge is to determine the optimal design configuration of the supersonic inlet geometry that maximizes engine performance while considering various aerodynamic factors. The researchers aim to understand the complex relationship between back pressure and shock wave positioning and its influence on the flow state within the intake.the intricate flow dynamics and their dependence on

design parameters and back pressure, the researchers aim to provide insights and guidelines for engineers working on supersonic inlet design in the aerospace industry.

4- Intake design

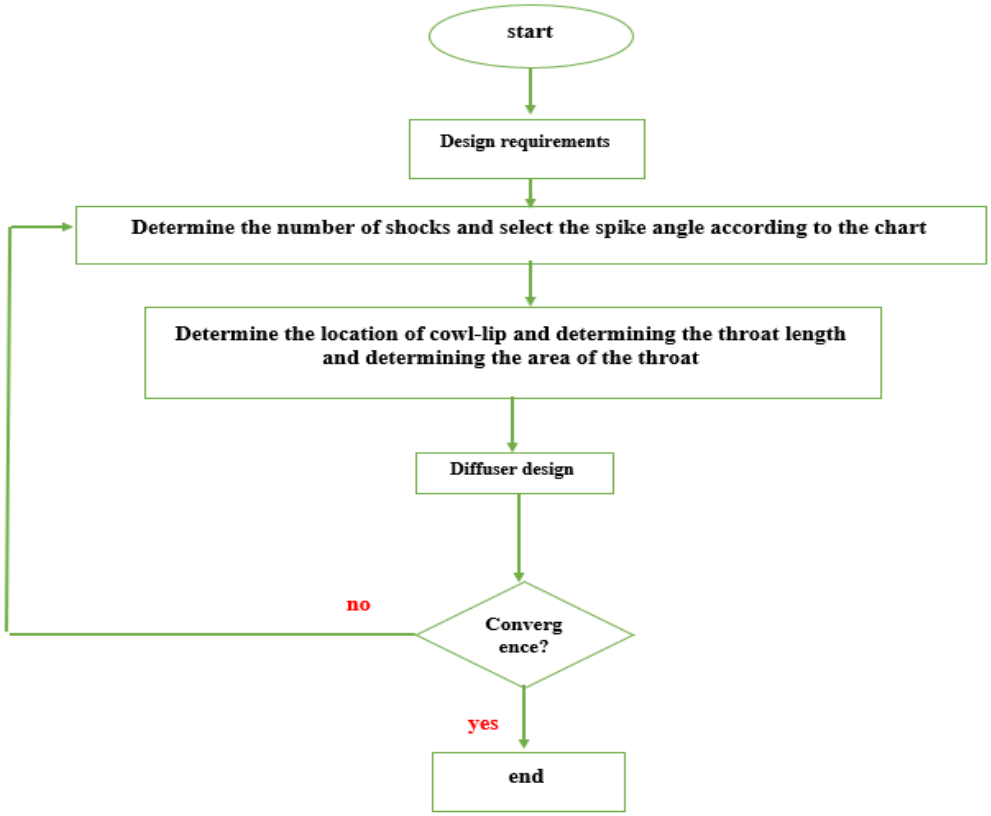

A)

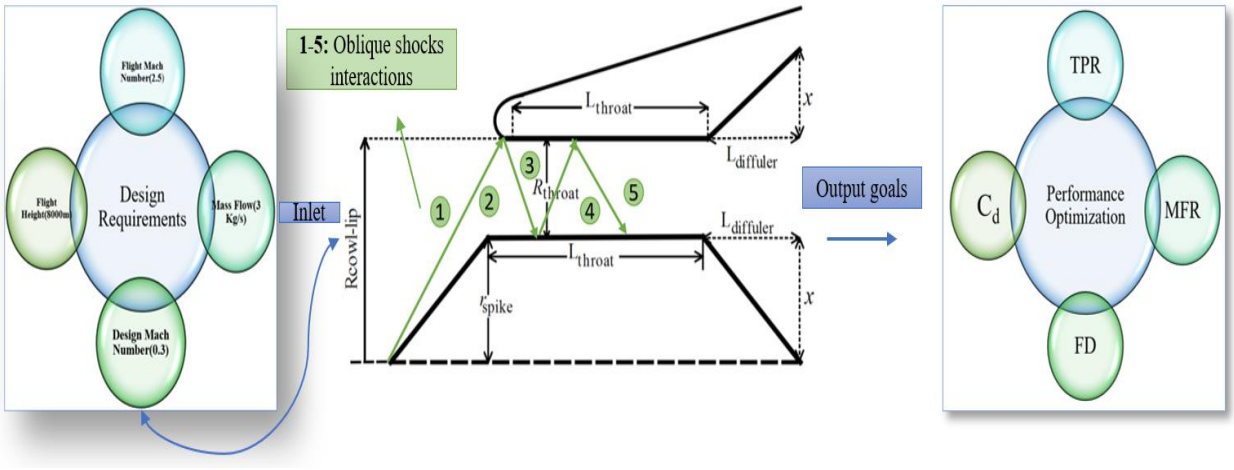

B)

Fig 1. A) Flowchart used in design and intake testing. B) Schematic of research geometry and final purpose.

Figure 1 shows an overview of the problem probe, A) shows the process of solving and convergence, and B) shows a view of the input and the goal of solving the problem.

4-1 Design requirements

The mendatory design requierments are available in Table 1

Table 1- Design requirements

Flight Height (m)	Mass flow (Kg/s)	The number of the intake ends	Mach number flight
8000	3	0.3	2.5

4-2 Determining the number of inclined shocks at the front intake

In Figure(2) to reduce the waste and have the highest efficiency due to the input Mach (2.5), it is used in Figure 2 of 2 shocks for the front of the intake.

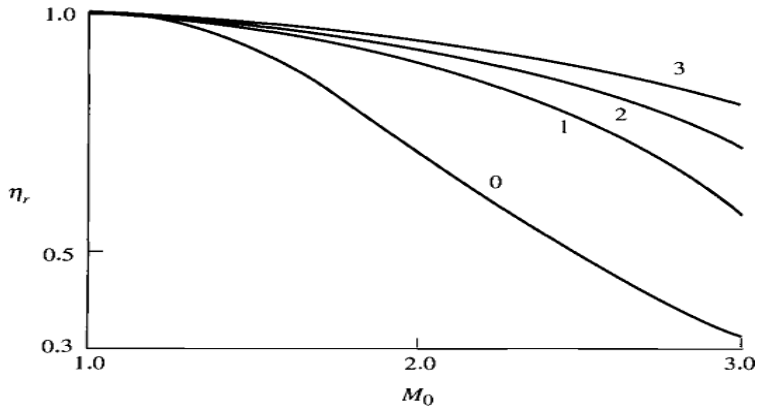

Fig 2. Intake efficiency Diagraph in terms of the number of shocks[27]

4-3 Determination of spike angles

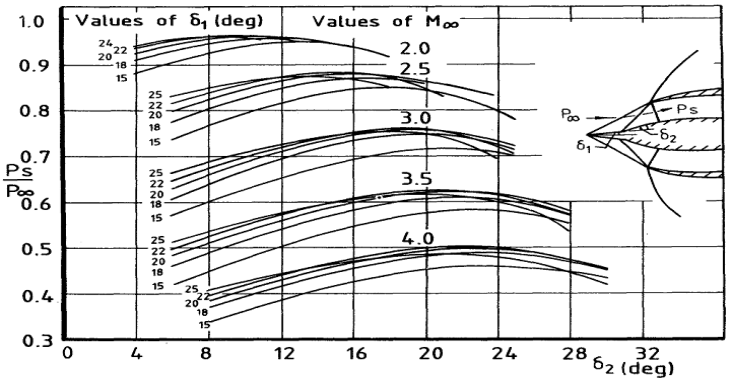

Fig 3. Graph of pressure ratio by spike angle[27]

In Figure 3, according to the input Mach, the first angle is considered 16 degrees to have the highest efficiency, and in this design, the second angle is also considered 16 degrees(To further reduce the loss and placement of shock in the inlet intake).

4-4 Cowl-Lip location determination

First, according to the input conditions and Table Standard Atmosphere, the temperature, pressure, density, and speed of sound have been determined

$h = 8000$

$M = 2.5$

$\dot{M} = 3$

$M_e = 0.3$

$P_\infty = 35599.8$

$T_\infty = 236.15$

$\rho_\infty = 0.525$

$a_\infty = 308.063$

These values were read from the standard atmosphere table for an altitude of 8000 meters

According to the Mach number of the incoming flow and the isentropic table:

$P/P_0 = 0.05852 \rightarrow P_o = 608335.6118$

$T/T_0 = 0.444 \rightarrow T_o = 531.8693694$

Using equation (1), speed has been obtained

$$V = M \times a \tag{1}$$

Equations (2)and (3)have been used to determine the transverse coordinates of Cowl Lip[27].

$$R_{Cowl-Lip} = \sqrt{\frac{\dot{m}}{\rho \pi v}} \tag{2}$$

$$A_{Cowl-Lip} = \pi R^2 \tag{3}$$

$R_{Cowl\text{-}Lip}$: This represents the transverse coordinate or radius of the Cowl Lip.

$\dot{m}$: It stands for the mass flow rate, which is the amount of mass passing through a specified point per unit time.

$A_{Cowl-Lip}$: This represents the area of the Cowl Lip, which is the surface area enclosed within the defined boundary.

Determining the longitudinal coordinates of Cowl -Lip using the beta angle code, we derive equation (4)for the following specifications.

$$\begin{cases} M = 2.5 \\ conical - Angle = 16 \end{cases} \rightarrow \beta = 29.256192$$

$$X_{Cowl-Lip} = \frac{R_{CL}}{Tan(\beta)} \tag{4}$$

4-5 Determining the area of the throat

To determine the area of the throat, equation (5)is used, where A and B are constant values, and M is the input Mach[19].

$$\frac{A_{Cowl-Lip}}{A_{th}} = A + BM_1 (A = 1.12396722, B = 9.948786E - 2) \tag{5}$$

A_{th}: The value or area represented by A_{th} corresponds to the area of the throat.

A and B: These are constant values used in the equation. In this case, A is equal to 1.12396722 and B is equal to 9.948786E-2.

4-6 Determine the location of the spike

Equations (6), (7), and (8) have been used to determine the location of the spike[27].

$$A_{spike} = A_{Cowl-Lip} - A_{th} \tag{6}$$

$$r_{spike} = \sqrt{\frac{A_{Cowl-Lip}}{\pi}} \tag{7}$$

$$X_{spike} = \frac{r_{spike}}{Tan(\delta)} \tag{8}$$

A_{spike}: The value represented by A_{spike} corresponds to the area of the spike.

r_{spike}: This represents the distance from the centerline to the outer edge of the spike.

X_{spike}: This represents the location or position of the spike.

4-7 Determining the length of the throat

Equation (9)is used to determine the size of the throat[27].

$$L_{th} = 4.\left(r_{Cowl-Lip} - r_{spik}\right) \tag{9}$$

L_{th}: The value represented by L_{th} corresponds to the length or size of the throat.

4-8 Determine the end radius intake

Equations 10, 11, and 12 have been used to determine the end radius intake, but first of all, it is necessary to calculate the characteristics of the flow.

$$P_{t5} = \frac{P_{t4}}{P_{t3}} \times \frac{P_{t3}}{P_{t2}} \times \frac{P_{t2}}{P_{t1}} P_{t1} = 608335.6118 \times 0.990 \times .99674 \times 0.835469 = 501522.778$$

$$(P_{t4} = P_{t5})$$

$$1 \rightarrow 2 \xrightarrow{Normal\ shock\ Table} M_1 = 2.5, \theta_{conical} = 16 \rightarrow \begin{cases} \beta = 29.26 \\ M = 2.082 \\ \frac{Po_2}{Po_1} = 0.990 \end{cases}$$

$$2 \rightarrow 3 \xrightarrow{conical\ shock\ Table} \begin{cases} cone - angle = 16 \\ M_3 = 1.7479 \\ Po_3/Po_2 = 0.99674 \\ \beta = 33.4874 \end{cases}$$

$$3 \rightarrow 4 \xrightarrow{Normal\ shock\ Table} \begin{cases} M_4 = 0.6285 \\ M_3 = 1.7479 \\ \frac{Po_4}{Po_3} = 0.83546964 \end{cases}$$

$T_{t5} = T_{t1}$

***

$$MFP = \sqrt{\frac{\gamma}{R}}.Me\left(1 + \frac{\gamma - 1}{2} M^2\right)^{\frac{-(\gamma+1)}{(2\gamma-2)}} \quad (10)$$

$$A_5 = \frac{\dot{m}\sqrt{T_t}}{MFP \times P_{t5}} \quad (11)$$

$$r_5 = \sqrt{\frac{A_5}{\pi}} \quad (12)$$

MFP: Stands for "Mach number to Flow Perpendicular" and represents a characteristic quantity used in compressible flow calculations.

4-9 Determine the length of the diffuser

To determine the length of the diffuser, we use equations 13, 14, and 15; to calculate the total size of the intake, we use equation 16 [27].

$$r_{th} = R_{Cowl-Lip} - R_{Spike} \quad (13)$$

$$r_5 = r_{th} + 2X \quad (14)$$

$$L_{diffuser} = \frac{x}{\tan(3)} \quad (15)$$

$$\text{Total length Intake} = Xspike + L_{throat} + L_{diffuser} \quad (16)$$

5- Test Intake geometry

This test used an inlet with a length of 40.79 and an angle of 16 degrees. The overall dimensions of this inlet can be seen in Figure 4.

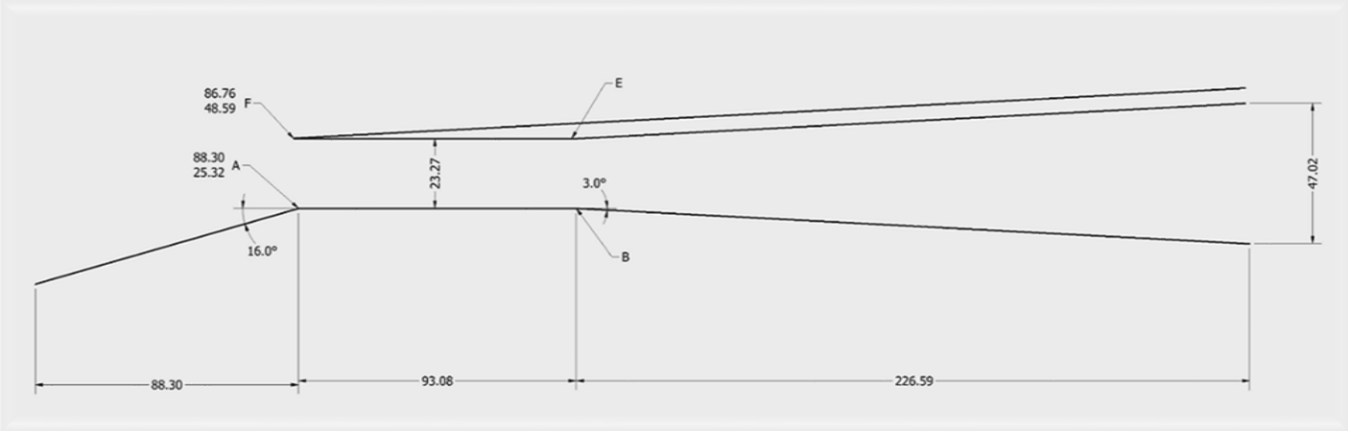

Fig 4. Intake of a two-dimensional image with dimensions(mm)

6- Solution method and domain

In this research, a simulation of the inlet flow has been done using computational fluid dynamics. The governing equations have been discretized and solved by the finite volume method. The flow solution has been implemented as a constant and base density. Due to the presence of reverse pressure gradient and flow separation on the inlet at different back pressures, the selected turbulence model has been used from the K-W-SST two-equation model. At the entrance, the turbulence intensity is equal to 2.4%, and the atmospheric conditions of the sea surface are applied in standard situations. The Reynolds number of this problem will equal 384848.6 according to the average chord length and flow conditions. The solution algorithm is of the Simple C type, which is used for pressure terms from the second-order scheme and other equations (momentum, losses, kinetic energy of turbulence) from the upstream second-order scheme.

6-1Mesh and independence from the mesh

Ansys Meshing software is used in mesh production. The elements created in this meshing are unorganized, along with the boundary layer mesh on the model's surface. To increase the accuracy in calculations and display the phenomena around the model, the mesh has been made smaller in an elliptical volume around the model. Also, despite the 1.2 times micro permeability coefficient, from far distances towards the intake and entrance walls, the dimensions of the elements are smaller, and the mesh volume has increased. In Figure 5, views of the mesh are created, and the boundary conditions and dimensions are significant. Figure 6 shows independence from the mesh. The created mesh is of unorganized type and was done by Ansys Meshing software. The mesh is finer as it gets closer to the walls and corners of the model. According to the choice of K-W-SST turbulence model, the dimensionless Y-plus number 1.3. Choosing this value for the Y-plus number is greater than one , according to references [28-29] has been accepted.

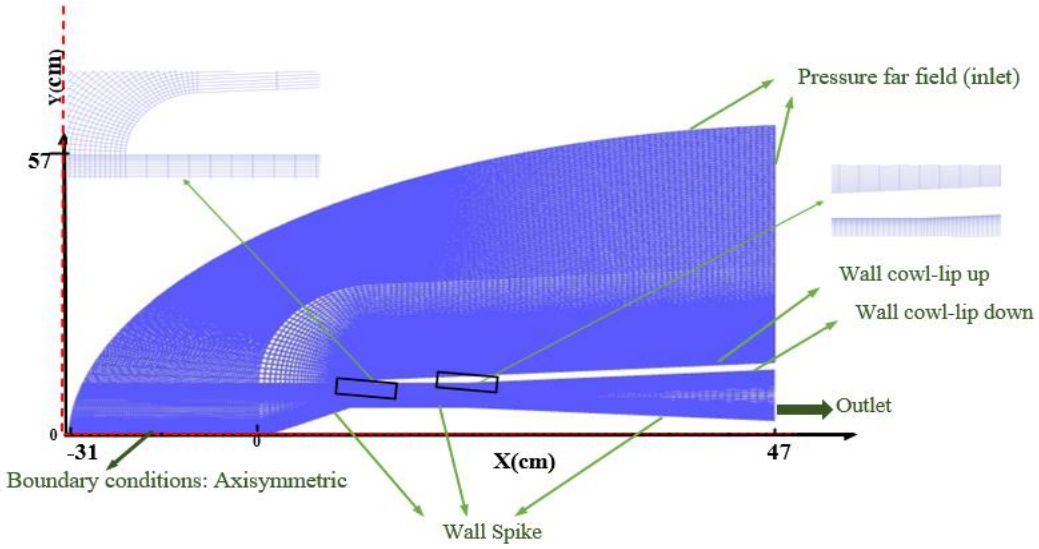

Fig 5. Boundary conditions and view of the mesh

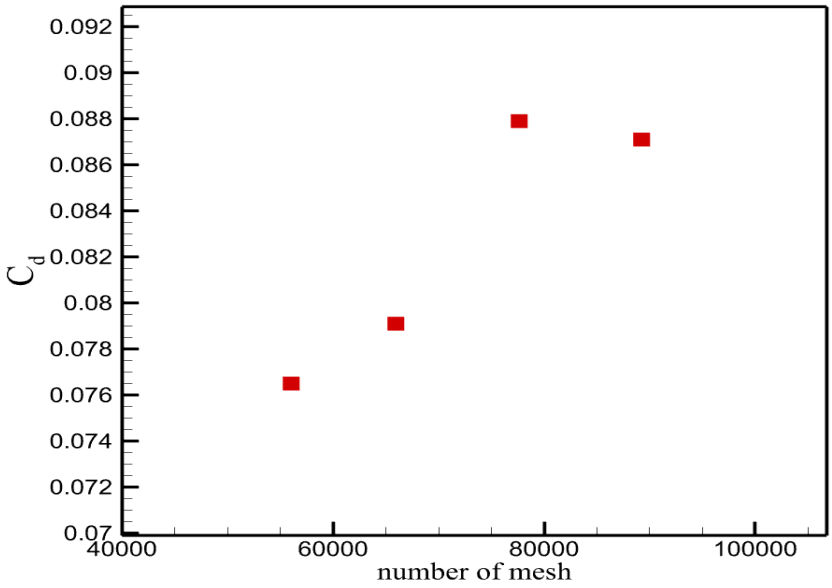

Fig 6. Independence from the network for the back pressure of 50,000 pascals in the wall of Cowl-Lip

7- Simulation results

In Figure 7, the shock is inside the diffuser, which moves towards the throat with the increase of the back pressure of the shock, which is called the supercritical state. As seen in Figure 8, with a further increase in the aftershock pressure, it travels the length of the throat, and this state is called the critical state. The crucial state in which the shock is located in the throat, in the correct position, and in addition to the design flow, and Mach is achieved, is reported in the range of back pressure of 300 to 350 thousand pascals. As shown in Figure 10, with a further increase in back pressure, the shock exits the throat, and the subcritical state occurs.

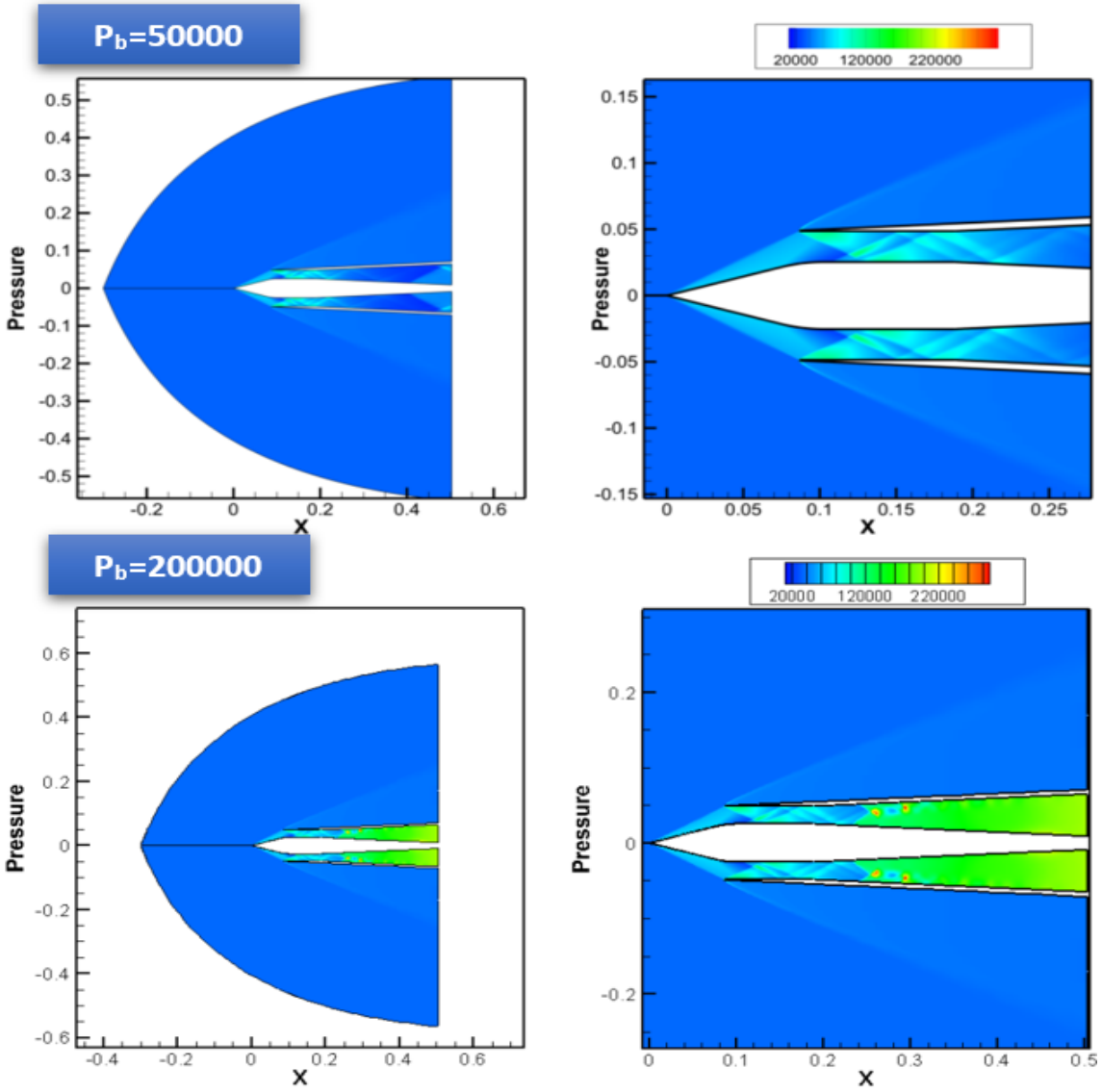

Fig 7. Pressure contour after pressures of 50,000 and 200,000 pascals

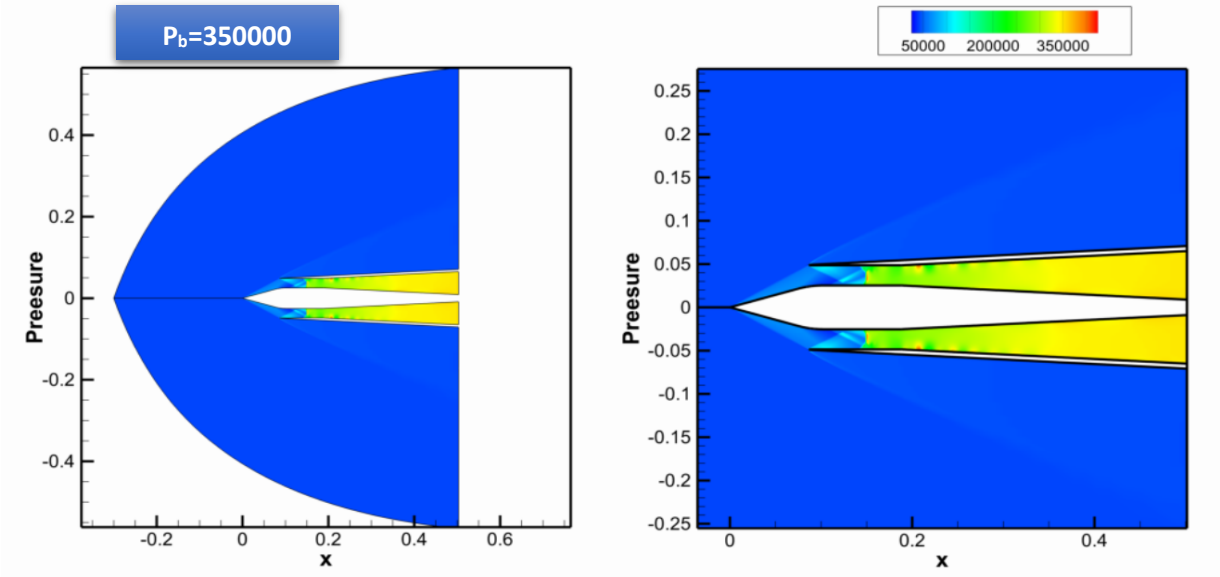

Fig 8. Pressure contour after pressures of 350000 pascals

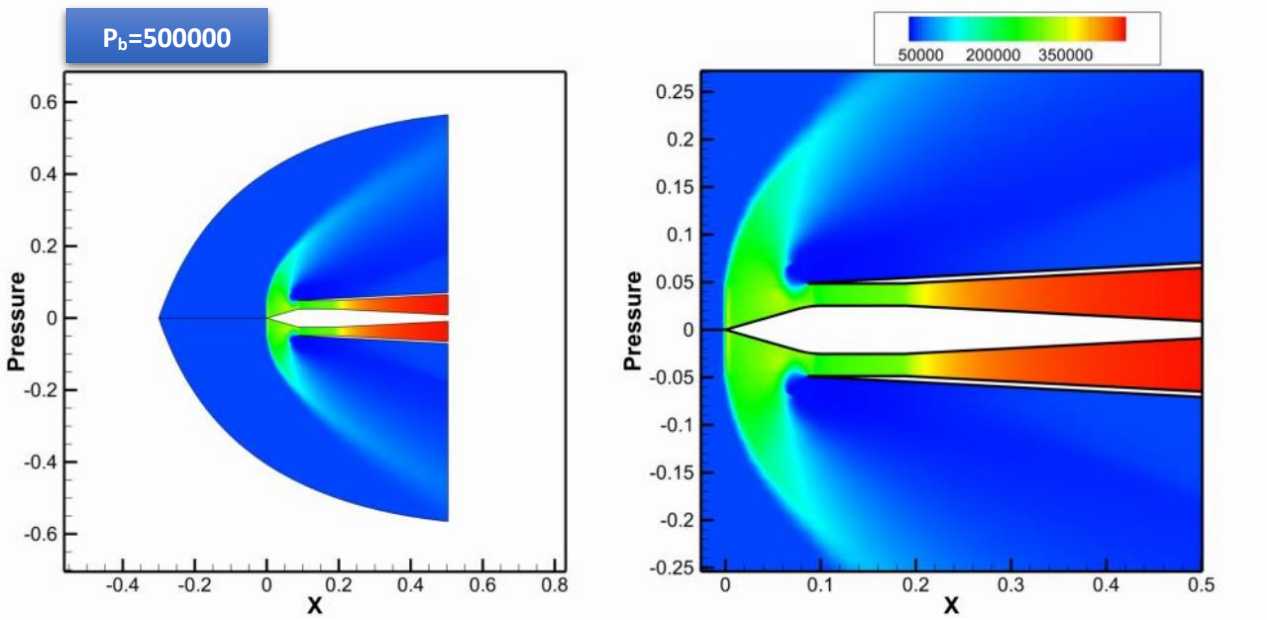

Fig 9. Pressure contour after pressures of 500000 pascals

In Figure 9, we will have a mass flow overflow due to exiting the SOL (Shock On Lip) state, and this problem becomes more severe with a further increase in back pressure. The amount of ultrasonic flow in the diffuser decreases with the rise in back pressure and the normal movement of the shock toward the throat; in the subcritical state, the entire area inside the inlet will be subsonic. In the diagram of Figure 10, the drag coefficient in terms of back pressure is given for nine different back pressures.

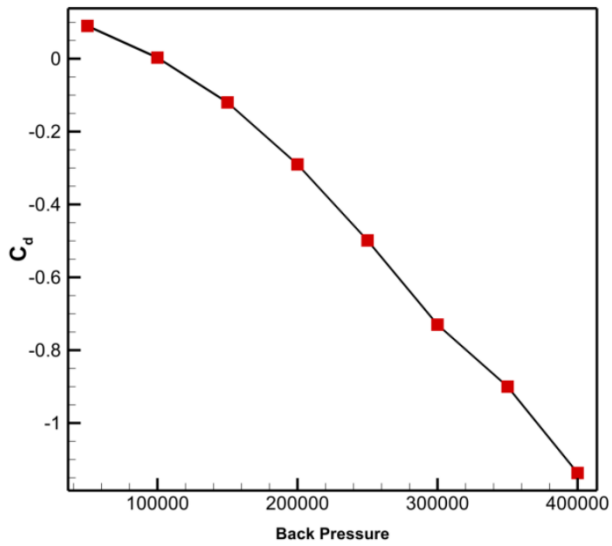

Fig 10. The diagram of the drag coefficient in terms of back pressure

The generation of back pressure reduces the drag coefficient. From the pressure coefficient of 150,000 onwards, the amount of pressure forces outside the inlet is less than the amount of pressure forces inside the inlet, and it creates a negative drag coefficient and helps to produce propulsive force.

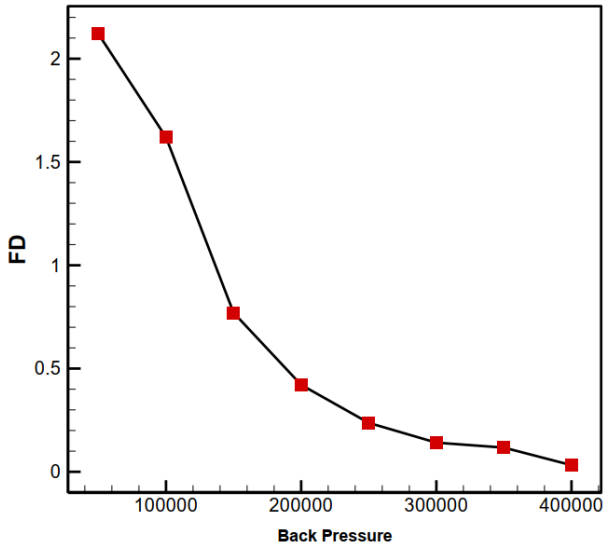

Fig 11. Intake distortion coefficient diagram under different back pressures

It can be seen in Figure 11 that the amount and amount of distortion has an inverse relationship with the back pressure. After the final pressure changes, the amount of distortion decreases; on the other hand, the most significant amount of distortion is after the initial pressures, and due to the high volume of separation in the diffuser, the normal movement of the shock towards the exit opening with an increase in back pressure leads to a reduction in distortion.

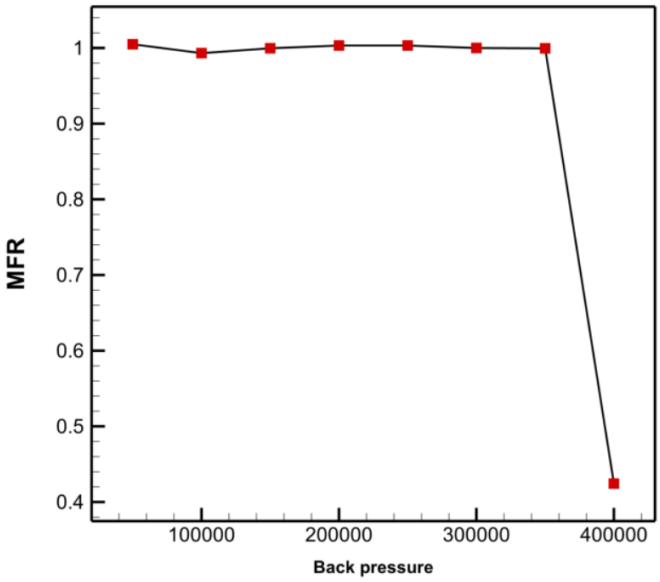

Fig 12. The graph of the input Mass Flow Ratio (MFR) at different back pressures

According to the diagram in Figure 12, it can be seen that in the subcritical state, because the shock is located precisely at the inlet opening, all the mass flow rate of the fluid enters the inlet, and the mass flow

rate ratio is almost equal to one. But the MFR value decreases as the back pressure increases and the shock is placed outside the opening and the flow overflows. The sudden decrease in the MFR can be justified by the significant reduction in the effective flow area due to flow separation. The flow separation creates additional pressure losses and disrupts the smooth entry of the fluid. Consequently, a smaller portion of the total mass flow rate manages to enter the inlet, resulting in a lower MFR value.

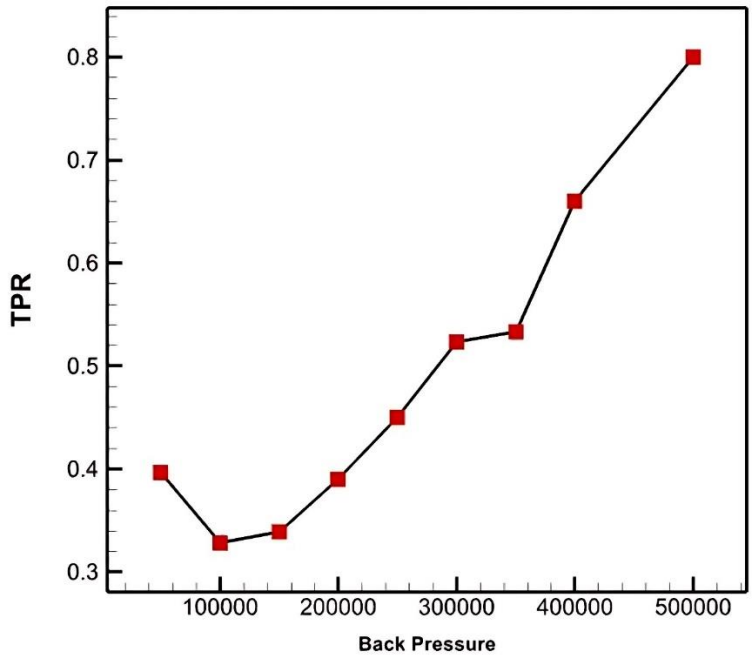

Fig 13. Recovery diagram of the total input pressure(TPR) at different back pressures

In Figure 13, it can be seen that the changes in total pressure recovery in terms of different back pressures have a linear relationship until the occurrence of the open phenomenon, and the increase in back pressure leads to an increase in total pressure recovery. In the supercritical region, with the rise in back pressure, the Mach number behind the shock will be smaller, leading to an increase in the recovery of the total force. The total pressure is increased. From a physical point of view, the minimum total pressure recovery (TPR) observed at a back pressure of 10000 can be explained by considering the impact of the shock wave and the behavior of the flow:

In the supercritical region, as the back pressure increases, the Mach number behind the shock wave decreases. This decrease in the Mach number leads to an increase in the recovery of the total pressure. Generally, higher total pressure recovery is observed with higher back pressures. However, at a specific back pressure of 10000, a minimum TPR occurs. This can be attributed to the interaction between the incident flow and the shock wave. When the back pressure is at a certain value, the shock wave configuration and position undergo a significant change. The shock wave may become stronger or more oblique, affecting the flow behavior and leading to an adverse impact on the total pressure recovery. One possible physical explanation for the minimum TPR at a back pressure of 10000 is that the shock wave configuration becomes unfavorable for efficient total pressure recovery. It could result in increased losses, such as stronger shock wave dissipation or stronger turbulence generation at the shock wave boundary. These adverse effects can disrupt the smooth flow passage and cause a reduction in the total pressure recovery. As a result, the TPR value drops to a minimum level at this specific back pressure.

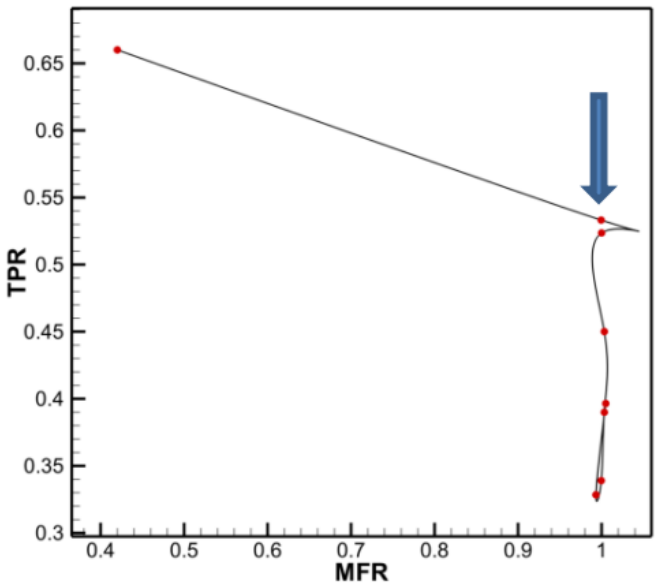

Fig 14. Intake functional diagram

In the mentioned critical range, the best performance is observed for the input, which means that in this range, both the optimal mass ratio and the optimal pressure recovery of the intake have been achieved. However, in other cases, a higher mass ratio or pressure recovery may be observed, but the most favorable state is the optimality of both parameters in the obtained critical range, which can be seen in Figure 14.

8-Conclusion

In conclusion, this research paper focuses on the preliminary aerodynamic design of a ramjet inlet duct for a Mach 2.5 flight under specific design conditions. The design process involves determining various parameters such as the number of shocks at the front intake, spike angles, cowl-lip location, throat area, spike location, length of the throat, and end radius intake. Computational fluid dynamics (CFD) simulations were performed to analyze the flow behavior and performance of the intake geometry. The results show that the intake design operates in three states: supercritical, critical, and subcritical, depending on the back pressure. In the supercritical state, the shock is inside the diffuser and moves toward the throat with increasing back pressure. In the critical state, the shock is correctly positioned in the throat, achieving design flow and Mach conditions. The subcritical state occurs when the shock exits the throat, leading to mass flow overflow and reducing intake performance. The simulations also revealed that increasing back pressure reduces the drag coefficient, and a negative drag coefficient can be achieved, contributing to propulsive force generation. The distortion coefficient of the intake decreases with higher back pressures due to reduced separation and improved shock movement. The mass flow ratio drops as the shock moves outside the opening and the flow overflows. The total pressure recovery shows a linear relationship with back pressure until the open phenomenon occurs, resulting in increased

recovery. Overall, the research provides insights into the aerodynamic design and performance of ramjet entry ducts, highlighting the importance of optimizing various parameters to achieve efficient intake operation. The findings contribute to understanding intake flow behavior and can guide future design improvements in supersonic propulsion systems.

Data availability

The datasets generated during and/or analysed during the current study are not publicly available due to regulations of our supervisor affiliation but are available from the corresponding author on reasonable request.

9-Reference

[1] Yadegari, M. and M. Jahdi, Capturing of Shock Wave of Supersonic Flow over the Bump Channel with TVD, ACM and Jameson Methods. Iranian Journal of Mechanical Engineering Transactions of the ISME, 2021. 22(1): p. 108-126.

[2] Yadegari, M. and M. Abdollahi Jahdi, Shock capturing method by numerical dissipation control on symmetric airfoil. Journal of Solid and Fluid Mechanics, 2016. 6(1): p. 285-304.

[3] Yadegari, M. and A. Bak Khoshnevis, Investigation of entropy generation, efficiency, static and ideal pressure recovery coefficient in curved annular diffusers. The European Physical Journal Plus, 2021. 136: p. 1-19.

[4] Yadegari, M. and A.B. Khoshnevis, Entropy generation analysis of turbulent boundary layer flow in different curved diffusers in air-conditioning systems. The European Physical Journal Plus, 2020. 135(6): p. 534.

[5] Yadegari, M. and A.B. Khoshnevis, Numerical study of the effects of adverse pressure gradient parameter, turning angle and curvature ratio on turbulent flow in 3D turning curved rectangular diffusers using entropy generation analysis. The European Physical Journal Plus, 2020. 135(7): p. 548.

[6] Yadegari, M., An optimal design for S-shaped air intake diffusers using simultaneous entropy generation analysis and multi-objective genetic algorithm. The European Physical Journal Plus, 2021. 136(10): p. 1019.

[7] Yadegari, M. and A. Bak Khoshnevis, A numerical study over the effect of curvature and adverse pressure gradient on development of flow inside gas transmission pipelines. Journal of the Brazilian Society of Mechanical Sciences and Engineering, 2020. 42: p. 1-15.

[8] Haghighatjoo, H., M. Yadegari, and A. Bak Khoshnevis, Optimization of single-obstacle location and distance between square obstacles in a curved channel. The European Physical Journal Plus, 2022. 137(9): p. 1042.

[9] Goldsmith EL, Seddon J. Practical intake aerodynamic design. (No Title). 1993 Nov.

[10] Sepahi-Younsi, J., Forouzi Feshalami, B., Maadi, S.R. and Soltani, M.R., 2019. Boundary layer suction for high-speed air intakes: A review. Proceedings of the Institution of Mechanical Engineers, Part G: Journal of Aerospace Engineering, 233(9), pp.3459-3481.

[11] Akbarzadeh M, Kermani MJ. Numerical Computation of Supersonic-Subsonic Ramjet Inlets; a Design Procedure. In15th. Annual (International) Conference on Mechanical Engineering-ISME2007 May 2007 (pp. 15-17).

[12] Gokhale SS, Kumar VR. Numerical computations of supersonic inlet flow. International journal for numerical methods in fluids. 2001 Jul 15;36(5):597-617.

[13] Duncan B, Thomas S. Computational analysis of ramjet engine inlet interaction. In28th Joint Propulsion Conference and Exhibit 1992 Jul 1 (p. 3102).

[14] Salmi RJ, Stitt LE. Performance of a mach 3.0 external-internal-compression axisymmetric inlet at mach numbers from 2.0 to 3.5. 1960 Jan 1.

[15] Syberg J, Paynter G, Carlin C. Inlet design technology development-Supersonic cruise research. In17th Joint Propulsion Conference 1981 Jul 1 (p. 1598).

[16] Howlett D, Hunter L. A study of a supersonic axisymmetric spiked inlet at angle of attackusing the Navier-Stokes equations. In24th Aerospace Sciences Meeting 1986 (p. 308).

[17] Rodriguez D. Multidisciplinary optimization of a supersonic inlet using a Cartesian CFD method. In10th AIAA/ISSMO Multidisciplinary Analysis and Optimization Conference 2004 (p. 4492).

[18] Zuo F, Huang G, Xia C. Investigation of internal-waverider-inlet flow pattern integrated with variable-geometry for TBCC. Aerospace Science and Technology. 2016 Dec 1; 59:69-77.

[19] Sorensen NE, Latham EA, Smeltzer DB. Variable geometry for supersonic mixed-compression inlets. Journal of Aircraft. 1976 Apr;13(4):309-12.

[20] Seddon J, Goldsmith EL, editors. Practical intake aerodynamic design. American Institute of Aeronautics and Astronautics; 1993.

[21] Lu PJ, Jain LT. Numerical investigation of inlet buzz flow. Journal of Propulsion and Power. 1998 Jan;14(1):90-100.

[22] Goldsmith EL, Griggs CF. The estimation of shock pressure recovery and external drag of conical centre-body intakes at supersonic speeds.

[23] Ran H, Mavris D. Preliminary design of a 2D supersonic inlet to maximize total pressure recovery. InAIAA 5th ATIO and16th Lighter-Than-Air Sys Tech. and Balloon Systems Conferences 2005 Sep 26 (p. 7357).

[24] Fujii, M., Ogura, S., Sato, T., Taguchi, H., Hashimoto, A. and Takahashi, T., 2022. Effect of angle of attack on the performance of the supersonic intake for High Mach Integrated Control Experiment (HIMICO). Aerospace Science and Technology, 127, p.107687.

[25] Koval, S., 2021. Analysis of Supersonic Axisymmetric Air Intake in Off-Design Mode. In Proceedings of the International Conference on Aerospace System Science and Engineering 2020 (pp. 43-53). Springer Singapore.

[26] Khobragade, N., Unnikrishnan, S. and Kumar, R., 2022. Flow instabilities and impact of ramp–isolator junction on shock–boundary-layer interactions in a supersonic intake. Journal of Fluid Mechanics, 953, p.A30.

[27] Haines AB. Intake Aerodynamics—Second edition. J. Seddon and EL Goldsmith. Blackwell Science, Osney Mead, Oxford OX2 0EL, UK. 1999. 1407pp. Illustrated.£ 59.50. ISBN 0-632-04963-4. The Aeronautical Journal. 2000 Feb;104(1032):96-.

[28] Moghimi Esfandabadi, M. H., Djavareshkian, M. H. (2023). 'Design and optimization of the wing fence of a lambda-shaped aircraft model to reduce the rolling moment coefficient', Technology in Aerospace Engineering, (), pp. 13-24. doi: 10.30699/jtae.2023.8.2.2

[29] Lakzian, E., Yazdani, S., Mobini, R., Abadi, M.H.M.E., Ramezani, A., Yahyazadeh, M. and Rashedi Tabar, M., 2022. Investigation of the effect of water droplet injection on condensation flow of different nozzles geometry. The European Physical Journal Plus, 137(5), p.613.